Morphology and Adhesion Strength in Electroless Cu Metallized AlN Substrate

J. H. Chang, J. G. Duh, and B. S. Chiou

***Abstract*— The metallization of aluminum nitride substrates by electroless copper plating is investigated. The AlN substrate is etched by 4% NaOH to study the correlation between the adhesion strength and the surface roughness of etched AlN substrate. Both the as-received nonpolished and then polished AlN are employed herein. For the nonpolished substrate, the adhesion strength increases from 130 kg/cm^2 for the sample with an average surface roughness of 0.2 μm to 230 kgf/cm^2 for the one with an average surface roughness of 0.82 μm. For the polished substrate, the adhesion strength reaches 271 kg/cm^2 with a surface roughness of 0.19 μm. Mechanical interlocking is the major cause for the adhesion strength between the Cu and AlN substrates. The polished substrate followed by etching could form fine cavities on the AlN surface, and the microetching effect results in a stronger mechanical interlocking, which increase the adhesion strength.**

I. Introduction

THE need for smaller and more reliable integrated circuits and the need for higher voltage device for power application are the trends of the electronics industry in recent years [1]. Alumina (Al_2O_3) ceramics have been widely used as substrate materials for high-speed, high-density circuits because of their high thermal conductivity [2]. Recently, aluminum nitride (AlN) ceramics have attracted much attention because of their higher thermal conductivity. The thermal conductivity of AlN is estimated to be 320 W/(m.k) for single crystals and 230 W/(m.k) for polycrystals. The thermal expansion coefficient is $4.3 \sim 4.6$, which is close to that of silicon [1], [3]. Since aluminum nitride exhibits excellent properties, it has become a potential material for improved performance in recent years [4].

Surface metallization is necessary for the application of electronic circuitry to ceramic substrates. Thin-film metallization with multiple metal layers, such as Ti–Pd–Au, Cr–Au, Cr–Cu, and TaN–Cr–Au [5], as well as printed thick-film, refractory-metal molybdenum (Mo–Mn) or tungsten (W), are conventional methods for metallizing ceramics [6]. Direct bond copper substrates are used mainly for high-power application because of the extremely low electrical resistance of the copper material, which allows extra large current in the conductors [7]. The electroless plating has many attractive features, such as excellent uniformity [8], precise control of thickness, process economy, the ability to plate on irregular or complex shapes, and selective plating to the discrete geometry of the substrate surface [9]–[11]. Electroless Cu plating renders an excellent approach to metallize the ceramic substrate, because of its low operational temperature, no requirement of applied circuit, and low cost [8], [9], [12]–[20]. Electroless plating to metallize insulating substrates generally requires a treatment of the surface to make it catalytic to initiate the deposition of metal from the electroless bath [20]–[26]. The most common preparation process is a two-stage treatment, in which the specimen is immersed first in a dilute stannous chloride solution, and then in a dilute palladium chloride solution [20]–[23]. Another commonly used catalyst is the one-component tin–palladium colloid. The colloidal solution is usually prepared by adding palladium chloride ions [24]–[26]. The reduction of Pd^{+2} by Sn^{+2} produces the colloidal particles that are adsorbed into the board surface by electrostatic force. The etched holes on the substrate render a mechanical interlocking between electroless Cu and substrate, which would increase the adhesion strength of electroless Cu [27]. Electroless plating on Al_2O_3 has been studied by several investigators [28]–[31]. The adhesion of electroless copper-plated Al_2O_3 demonstrated no loss of adhesion when exposed to high-temperature storage or cycling [32]. For soldered electroless copper-plated Al_2O_3, the copper–tin intermetallic dominated the mechanical performance due to crack initiation in the intermetallic region formed during high-temperature exposure [32], [33]. Although Al_2O_3 ceramic surfaces are usually very difficult to etch, the new AlN ceramic is etched easily by NaOH solution. The AlN surface can be etched to produce anchoring holes effectively, which give a higher adhesion strength. The adhesion of electroless Ni–P-plated AlN is a function of surface roughness (Ra) with NaOH etching solution [34]. Osaka *et al.* investigated the adhesion strength between Al ceramics and electroless plated Ni–P film from the viewpoint of the chemical etching behavior [35]. The first etching stage was due to the selective dissolution of the sintering-added Ca atoms, which was preferably proceeded along the triple points of the AlN grains. At the second etching stage, the AlN grains began to be etched and the adhesion strength gradually decreased with an increase in the dissolved amount of the AlN substrate.

A previous study by Chiou *et al.* reported the variation of adhesion between electroless Cu and AlN substrates [36]. In this study, the AlN substrate is etched by 4% NaOH to investigate the correlation between the adhesion strength and surface roughness of etched AlN substrates. The morphologies

Manuscript received July 27, 1992; revised June 4, 1993. This work was supported by the National Science Council, Taiwan, under Contract NSC 81-0404-E-009-610.

J. H. Chang and J. G. Duh are with the Department of Materials Science and Engineering, National Tsing Hua University, Hsinchu, Taiwan.

B. S. Chiou is with the Institute of Electronics, National Chaio Tung University, Hsinchu, Taiwan.

IEEE Log Number 9211648.

0148–6411/93$03.00 © 1993 IEEE

TABLE I
COMPOSITION OF ELECTROLESS Cu PLATING

	Chemical	Concentration
Sensitization	$SnCl_2 \cdot 2H_2O$	16 g/l
	HCl	30 ml/l
Activation	$PdCl_2$	0.1 g/l
	HCl	8 ml/l
Electroless Cu	$CuSO_4 \cdot 5H_2O$	30 g/l
	$KNaC_4H_4O_6 \cdot 4H_2O$	50 g/l
	EDTA	10 g/l
	HCHO (37%)	(a) 30 ml/l
		(b) 166 ml/l
	pH = 12.5 (adjusted by NaOH)	
	$T = 25° C$	

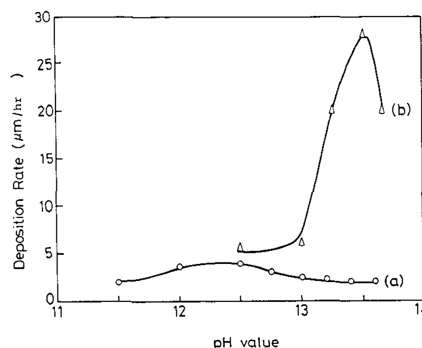

Fig. 2. Deposition rate of electroless Cu at various pH values: (a) low HCHO concentration (30 ml/l) bath; (b) high HCHO concentration (166 ml/l) bath.

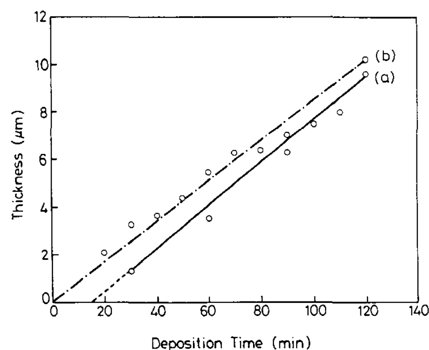

Fig. 1. Thickness of electroless Cu after different deposition times for pH = 12.5: (a) low HCHO concentration (30 ml/l) bath; (b) high HCHO concentration (166 ml/l) bath.

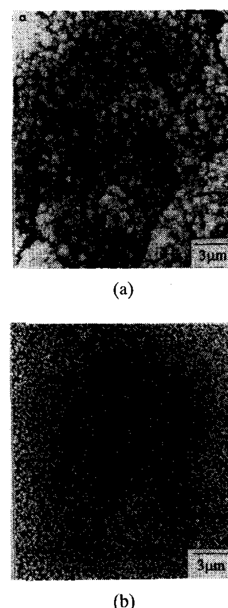

Fig. 3. Surface morphology of electroless Cu on AlN substrate: (a) non-polished substrate; (b) polished substrate.

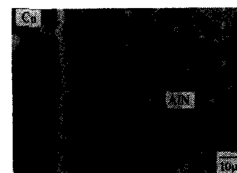

Fig. 4. Cross-sectional view of electroless Cu on AlN substrate.

of the as-deposited and fracture surface of the electroless Cu metallized AlN substrate are illustrated with the aid of electron microscopy. The relationship between microstructure and adhesion strength is discussed.

II. EXPERIMENTAL PROCEDURE

Aluminum nitride substrates 25.4 × 25.4 × 0.635 mm in size was abraded sequentially with 120, 400, 600, 1000, and 1200 grit SiC papers. After abrading, the substrate was polished through 6-, 3-, and 1-μm diamond pastes. The polished aluminum nitride substrate first was cleaned with ultrasonic rinsing in water for 5 min at room temperature, followed by ultrasonic cleaning in ethyl alcohol. The sample was then cleaned ultrasonically in water. After cleaning, the substrates were etched in 4% NaOH solution at room temperature for various times. The etched sample was then cleaned ultrasonically in water. The surface roughness of the etched substrates was measured with an α-step (ALPHA-STEP 250, Tencor, U.S.A.). The etched substrate was immersed in sensitization solution for 10 min. The compositions of sensitization solution are listed in Table I. After sensitization, the sample was appropriately rinsed with D.I. water. The sample was then immersed in the activation solution for 5 min. The composition of activation solution is also listed in Table I. The substrate should be rinsed appropriately with D.I. water before electroless copper plating.

The composition of the electroless copper bath is also represented in Table I. Among the chemicals employed for electroless copper plating. HCHO acts as the reducing agent to convert Cu^{2+}, which is derived from $CuSO_4$–$5H_2O$, back to the metal state Cu. NaK tartrate and EDTA, used as complexing agent, render part of Cu^{2+} to form complexants. The control of pH value is through the application of NaOH. The nitrogen gas that was introduced through a dispersed

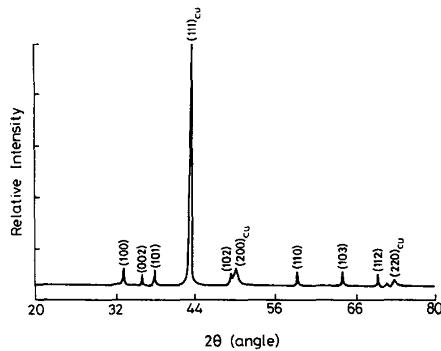

Fig. 5. X-ray diffraction pattern for electroless Cu deposition on AlN substrate.

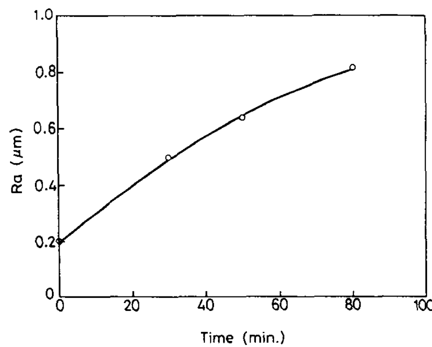

Fig. 6. Average surface roughness at various etching times for nonpolished AlN substrate.

pipe could eliminate the hydrogen gas, produced from the reaction of electroless copper plating, on the deposit surface. Another function of nitrogen is stirring the solution, which could regulate the decreased concentration of reactants on the deposit. The magnetic stirrer was also applied to the solution. The as-prepared sample was held with two pieces of glass plates. The pretreated aluminum nitride substrate was immersed in an electroless Cu bath at room temperature. The work load was 0.32 dm^2/l. Deposition with small work load should not affect the deposition rate. The deposit thickness was controlled by the deposition time. The electroless Cu deposited substrate was rinsed with D.I. water, followed by drying. The thickness of the electroless Cu deposit was measured with an α step (ALPHA-STEP 250, Tencor, U.S.A.). The probe scanned through the step, then the difference in height between deposit and substrate was derived. The difference in height was the thickness of the deposit. The probe scanned through the step in ten different scanning lines. The thickness value of the deposit in each scanning line was averaged, and the thickness of the deposit was determined. The average surface roughness can also be measured with an α step. The arithmetic average roughness is determined using the graphical-centerline method. This reading can be used to compute roughness according to ANSI Standard B46.1-1978. However, for most

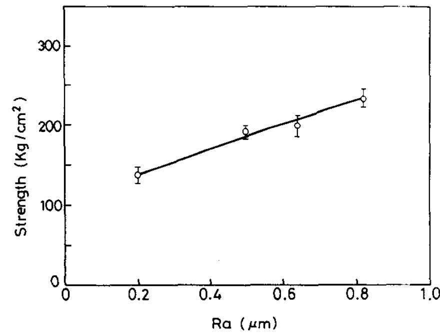

Fig. 7. Correlation between adhesion strength and surface roughness.

applications, the value displayed for Ra can be used directly, without additional computation. The phase and crystal structure were identified with a X-ray diffractometer (D/MAX-B, Rigaku, Japan) with a wavelength of Cu Kα (1.5406 A). The surface morphology and cross-sectional view morphology were analyzed with a scanning electron microscopy (SEM) (250 MK3, Cambridge, England) equipped with EDX (Excel, Link, England). A compositional depth profile was recorded by Auger electron spectroscopy (Perkin-Elmer PHI-590AM Scanning Auger Microprobe, Massachusetts, U.S.A.). The adhesion strength of Cu deposited on the AlN substrate is evaluated with a direct pull tester (Sebastian Five, Quad Group, U.S.A.). A stud was bonded perpendicularly to the coating surface with epoxy by holding it in contact through a spring mounting chip designed especially for the stud. The assembly was cured at 150° C for 1 h. The stud was inserted into the platen and gripped. The tester pulled the stud and samples down against the platen support ridge until the coating or epoxy failed. The force was increased slowly until failure occurred at F (kg). For the area A (cm^2) of the circular section of the stud, the stress of adhesion σ_a (kg/cm^2) is defined as $\sigma_a = F/A$.

III. Results and Discussion

To derive the deposition rate of electroless Cu on AlN substrate, the thickness of the deposit is measured with an α step. The measured thickness divided by deposition time is the deposition rate. For the low HCHO concentration (30 ml/l) bath at pH = 12.5, the thickness of electroless Cu after different deposition times is shown in Fig. 1(a). It is observed that Cu fails to adhere to the substrate before 5–6 min. After about 10 min, the copper covered the full substrate. Thus, there exists a retardation time to catalyze the electroless Cu reaction the substrate. After a thin layer of copper is deposited, the electroless Cu reaction can be catalyzed by the deposited copper itself. The deposit rate, 4.7 μm/h, could be determined from the slope of the fitting curve in Fig. 1(a).

For the high HCHO concentration (166 ml/l) bath at pH = 12.5, the Cu adhered to the substrate after only a few seconds. The thickness of the electroless Cu after different deposition times is shown in Fig. 1(b). Since the time to catalyze the electroless Cu reaction is very short, these data points could be extrapolated as a straight line through the original point.

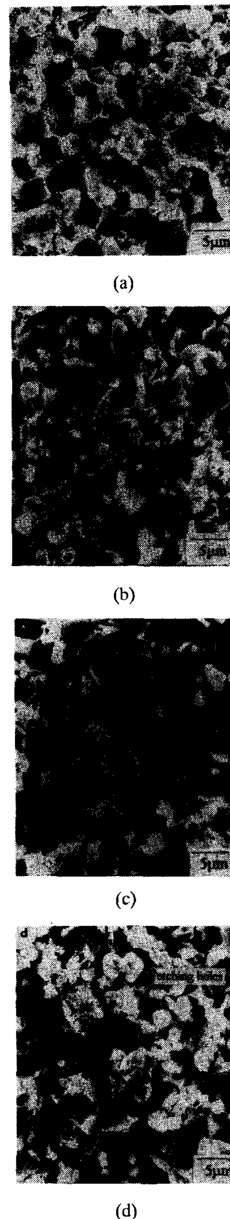

Fig. 8. Surface morphology of AlN substrate etched by 4% NaOH at various times: (a) 0 min; (b) 30 min; (c) 50 min; (d) 80 min.

The deposition rate, 5 μm/h, is derived from the slope of the fitted straight line in Fig. 1(b).

It should be pointed out that since the HCHO is used as a reducer, higher concentration of HCHO would have more driving force to initiate the electroless Cu reaction. This is why there exists a retardation time to initiate the electroless Cu reaction for the low HCHO concentration bath.

The deposition rate of electroless Cu on the HCHO substrate at various pH values is also investigated. Fig. 2(a) represents the dependence for low HCHO concentration (30 ml/l), whereas Fig. 2(b) is for high HCHO concentration (166 ml/l). The deposition rate reaches a maximum value at pH = 12.5 in the low HCHO concentration bath. However, for a high HCHO concentration bath, a maximum deposition rate of 28 μm/h occurs at pH = 13.5, above which the bath becomes unstable. The optimal pH values with respect to film integrity is 12.5, although the deposition rate is only 5 μm/h. It is argued that the gas formed on the deposit surface would be trapped in the deposit if the deposition rate is too fast. The presence of gas in the deposit tends to retard the electroless Cu deposition, and the electroless Cu reaction cannot proceed until the gas escapes the deposit surface. Higher concentration of HCHO results in more hydrogen gas formation, thus the porosity in the electroless deposit is increased.

A. Surface Morphology

The surface morphology of electroless Cu is shown in Fig. 3. Fig. 3(a) represents the surface morphology of electroless Cu on a nonpolished AlN substrate, in which some degree of agglomeration is observed. As for polished AlN substrate, deposited particles are well separated and uniformly distributed, as shown in Fig. 3(b). The cross-sectional view of electroless Cu on the AlN substrate is represented in Fig. 4. It should be noted that the deposition of electroless Cu depends on the chemistry of the substrate. Especially, it is sensitive to the active surface associated with the sensitization process. Thus, the electroless Cu tends to linerate the surface morphology of the substrate.

B. Microstructure Analysis

The composition of the electroless Cu deposit was analyzed by EDX. The cross-sectional sample of the electroless Cu was prepared. Only Cu is found in the X-ray spectrum, and a nearly pure copper state is assured. The X-ray diffraction pattern for electroless Cu deposition on the AlN substrate is shown in Fig. 5. The electroless Cu exhibits a primary (111) orientation. Peaks (200) and (220) are also found, but their intensities are rather low as compared with that of the (111) peak. The electroless Cu plating can be catalyzed by Cu itself, and the subsequent Cu is then deposited on the previously deposited Cu. As Cu is f.c.c. structure, the closed packed direction is (111). This explains the existence of (111) primary orientation in the deposited Cu film, as indicated in Fig. 5. The AES surface survey of the electroless Cu is carried out and elements Cu, O, C, and Cl are found in the film surface [37]. The Auger depth profile indicates a trace amount of oxygen, which results from oxidation of the electroless Cu surface, but the amount of oxygen is negligible. It should be pointed out that a detectable amount of chloride is observed near the surface. An appropriate cleaning approach should be employed to decrease the amount of chloride ion in the electroless Cu deposit.

C. Adhesion Strength

1) Surface Roughness Dependence: To roughen the substrate, the aluminum nitride substrate was etched with a 4% NaOH solution. In general, the average surface roughness (Ra) depends on the etching time. The average surface

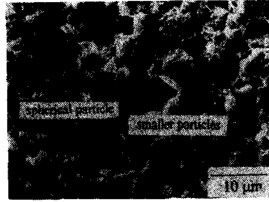

Fig. 9. Surface morphology of as-received AlN substrate.

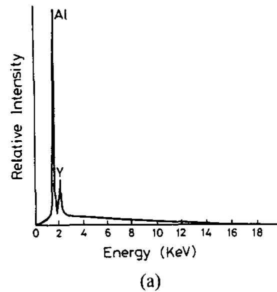

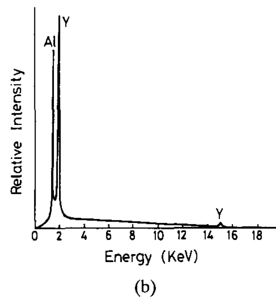

Fig. 10. EDX analysis of spherical particle: (a) substrate; (b) spherical particle.

roughness (Ra) at various etching times for the nonpolished AlN substrate is shown in Fig. 6. As the etching time is increased, the average surface roughness is enhanced. The average surface roughness of as-received AlN substrate is 0.2 μm, and the average roughness reaches 0.8 μm when the etching time is 80 min. The correlation between adhesion strength and surface roughness is represented in Fig. 7. The adhesion strength could reach 230 kgf/cm^2 as the surface roughness of the substrate is 0.8 μm. The surface morphology of etched substrate is shown in Fig. 8. Etching the substrate results in cavities that render the structure to form interlocking between substrate and electroless copper deposits, as seen in Fig. 8. Thus, the adhesion strength is increased.

In fact, interlocking structures are formed by selective etching by NaOH. Utsumi [34] argued that the intergranular small particles of the AlN substrate were etched selectively, and it was observed that the etching proceeded effectively to make the holes for the AlN substrate. In this study, as indicated in Fig. 9, small particles on the as-received substrate are observed. As the etching time increases, the regions that small particles occupy are etched selectively. Thus, holes are formed on the surface of the AlN substrate. It is also observed that some spherical particles are present in the deposit. EDX analysis indicates that this spherical particle is rich in Y, as shown in Fig. 10. It is believed that the enrichment of element Y results from the Y_2O_3 dopant in AlN for the enhancement of sintering [6]. Because the spherical particles are etched more slowly than the aluminum nitride matrix, a structure with spherical particles existing on the top of the specimen is found, as seen in Fig. 9. After the pull-off test, spherical particles are observed in the top of the fracture surface, as shown in Fig. 11. The presence of spherical particles on the fracture surface implies that the cracks propagate through the interface between the spherical particle and the underlying granular column when the pull-off test is applied. As a consequence, it is believed that the Y-rich spherical particle in the substrate plays an important role in the adhesion strength.

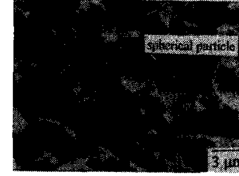

Fig. 11. SEM morhpology of fracture surface for electroless Cu-plated AlN after pull-off test.

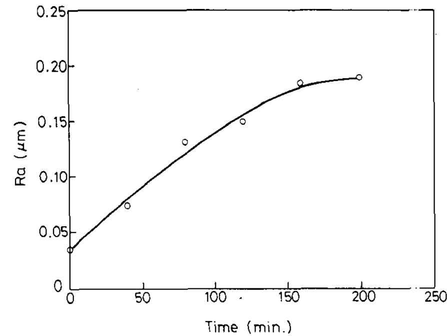

Fig. 12. Average surface roughness at various etching times for polished AlN substrate.

To have a smoother substrate surface, the substrate should be well polished. The average surface roughness of a polished substrate is only 0.035 μm. The polished substrates were also etched with 4% NaOH solution for various times. The average surface roughness for various etching times is given in Fig. 12; the surface morphology of etched substrates is shown in Fig. 13. The correlation between the adhesion strength and surface roughness for the polished substrate is represented in Fig. 14. As the substrate that is polished but not etched fails to provide sufficient interlocking structure on the substrate, the adhesion strength is only 49.5 kgf/cm^2. If the etching time is raised, some areas are etched selectively to form a small columnar structure. As the etching time is increased further, the amount of columnar structure appears to be increased. However, if the etching time is above 80 min, the amount of small columnar structures is decreased and larger cavities are introduced instead. Fig. 15 represents the morphology of the fracture surface after the pull-off test. It should be pointed out that a portion of copper is retained around the region etched on the substrate. This renders the copper and substrate

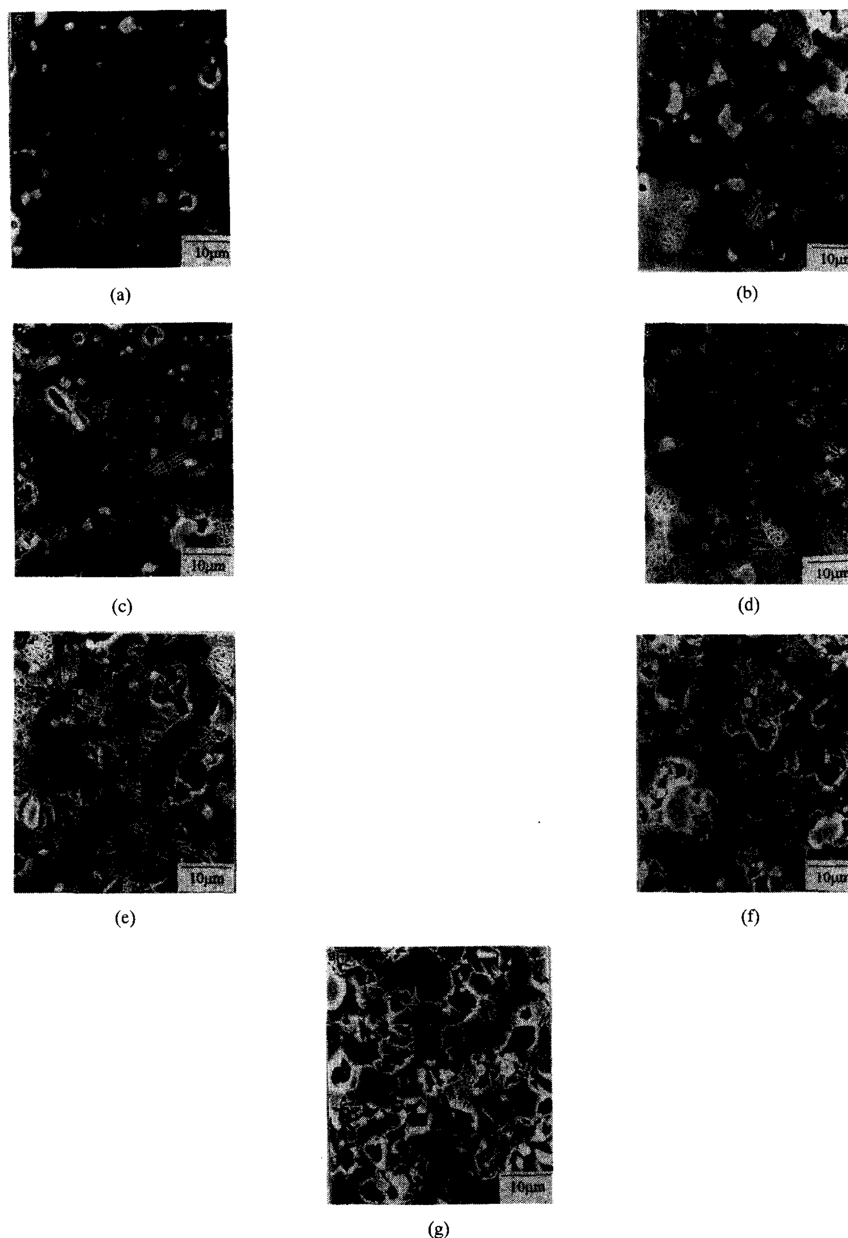

Fig. 13. Surface morphology of polished AlN substrate etched by 4% NaOH for various times: (a) 0 min; (b) 20 min; (c) 40 min; (d) 80 min; (e) 120 min; (f) 160 min; (g) 200 min.

to form an interlocking structure. The cross-sectional view of the electroless Cu-plated AlN substrate after the pull-off test is shown in Fig. 16. A portion of copper is retained on the substrate, and this copper is elongated. The ductility of the electroless copper might provide some degree of stress relaxation and results in enhanced adhesion strength. It is also argued that the plastic deformation associated with the ductile electroless copper tends to blunt crack propagation introduced during the pull-off test. Thus, the observed adhesion strength is increased.

In general, as the surface roughness increases, the surface area of the substrate in contact with the electroless copper is increased proportionally. Thus, the apparent adhesion strength is enhanced. Mechanical interlocking between the electroless copper and the AlN substrate could render mechanical bonding of the deposit on the substrate. Hence, the shape of the mechanical interlocking affects the measured adhesion strength. Etching the AlN substrate tends to form a hole that is broad at the bottom and narrow at the opening [38]. This structure renders a good mechanical bonding between

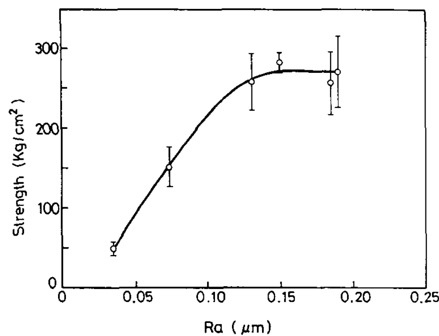

Fig. 14. Correlation between adhesion strength and surface roughness for polished AlN substrate.

TABLE II
ADHESION STRENGTH OF ELECTROLESS Cu ON AlN UNDER DIFFERENT PRETREATMENT

Sample	Pretreatment	Surface Roughness, Ra, μm	Adhesion Strength, kgf/cm^2
A	Nonpolished, no etching	0.20	137±10
B	Polished, etching 200 min	0.19	271±40
C	Nonpolished, etching 80 min	0.8	235±11
D	Polished etching, 80 min	0.13	259±35

the electroless copper film and the AlN substrate. Table II summarizes the measured adhesion strength of electroless Cu on the AlN substrate under various pretreatments. The substrate (i.e., sample B) etched longer and thus with enhanced surface roughness of 0.19 μm exhibits higher adhesion strength than the one etched lighter and with a surface roughness of 0.13 μm only (i.e., sample D). Although samples A and B have identical surface roughness, 0.20 μm and 0.19 μm, respectively, the measured adhesion strengths are different under different pretratment conditions. The adhesion strength of the substrate, polished and etched for 200 min, reaches 271 kgf/cm^2, which is much higher than that for the nonpolished and nonetched substrate (137 kgf/cm^2). Etching AlN substrate with 4% NaOH solution not only roughens the substrate surface but also forms a mechanical interlocking structure. Thus, the adhesion strength for the sample, polished followed by etching for 200 min, is much higher than that for the nonpolished and nonetched sample. It is believed that the polished substrate followed by etching exhibits finer holes than the nonpolished substrate followed by etching. The microetching structure, as seen in Fig. 13, could form a microinterlocking effect between the electroless copper and the AlN substrate. This type of microetching structure should exhibit better mechanical bonding than the structure with bigger holes, as seen in Fig. 8. Thus, the adhesion strength for the substrate with the microetching structure is larger than that for the substrate with a bigger hole structure. It is observed that the surface roughness of polished substrate increases from 0.035 to 0.13 μm after 80 min of etching, whereas that of the nonpolished substrate increases from 0.2 to 0.8 μm. The nonpolished substrate is etched more deeply than the polished sample, because there exist fewer weak sites for the polished substrate than the rougher surface of the nonpolished substrate. Thus, the polished substrate followed by etching could possess the microetching structure, which renders a more effective mechanical interlocking than the nonpolished substrate. This explains why the polished substrate D exhibits better adhesion strength than the nonpolished substrate C after identical etching treatment.

2) Thickness Dependence: As the deposit is applied on the substrate, the stress is introduced to the deposit. The stress on the deposit tends to increase if the thickness of the deposit is increased. The high level of concentrated stress in the deposit, which represents a great deal of absorbed energy by the deposit, would cause the crack to propagate. Thus, the adhesion strength between deposit and substrate decreases if the thickness comes into effect.

The adhesion strength of electroless copper with various thicknesses on the AlN substrate is shown in Fig. 17. It is observed that the adhesion strength decreases as the thickness of the electroless copper increases. The adhesion strength is around 800 kg/cm^2 at 3-μm thickness and decreases to 250 kgf/cm^2 if the thickness is larger than 10 μm. One was not able to measure the adhesion strength as the thickness of the electroless copper is as low as 1 μm, since the sample broke at substrate after the pull-off test. It is argued that the value for 1-μm electroless copper could reach 1000 kgf/cm^2, but this value does not represent the true value of the adhesion strength between the electroless copper and the AlN substrate. It should be pointed out that the electroless copper fails to cover the substrate completely if it is too thin. The epoxy used to adhere the sample and the stud for the pull-off test might adhere the deposit surface and the underlying substrate. Thus, a portion of the increased strength is attributed to the strength of the substrate itself, and an unusually high adhesion strength is recorded for a 1-μm electroless copper deposit. These data are, however, discarded in Fig. 17.

IV. SUMMARY AND CONCLUSIONS

The electroless Cu applied on the AlN substrate in the metallization process exhibits a (111) orientation since the (111) is the lowest energy direction for an f.c.c. structure and the autocatalytic characteristic of electroless plating. The deposition rate of electroless Cu on the AlN substrate is dependent on the pH value. The deposition rate reaches a maximum value and then decreases as the pH value is increased further. There exists a period of retardation time to initiate the electroless Cu plating on the AlN surface. After a thin layer of Cu is deposited, the electroless Cu reaction can be catalyzed by the deposited Cu itself.

Etching AlN substrate with a 4% NaOH solution creates holes that render the electroless Cu and AlN substrate to form mechanical interlocking. The adhesion strength of the electroless Cu on the AlN substrate increases if the surface roughness of the AlN substrate is enhanced. The polished AlN substrate followed by etching could form finer holes on the AlN substrate surface; these finer holes form a stronger

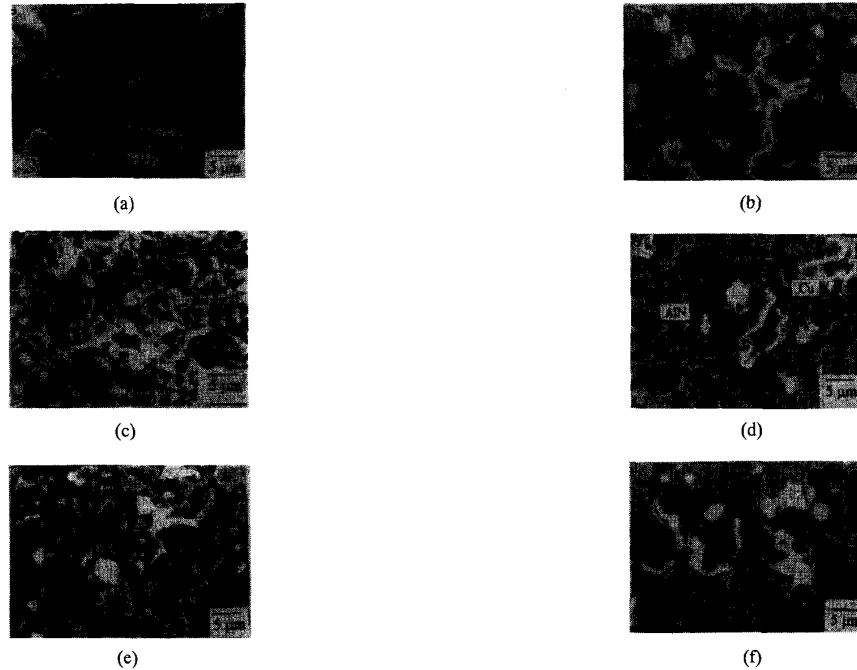

Fig. 15. Morphology of fracture surface after pull-off test. The AlN substrate is etched for various times: (a) 0 min; (b) 40 min; (c) 80 min; (d) 120 min; (e) 160 min; (f) 200 min.

Fig. 16. Cross-sectional view of electroless Cu-plated AlN substrate after pull-off test.

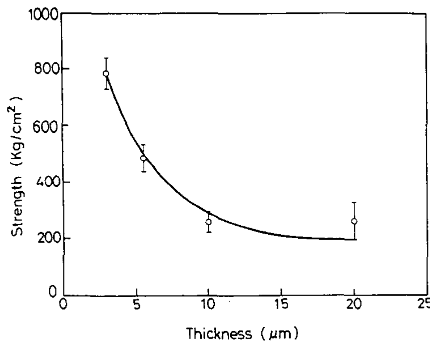

Fig. 17. Correlation between thickness of electroless Cu and adhesion strength on AlN substrate.

mechanical interlocking, and the adhesion strength is thus increased.

REFERENCES

[1] L. M. Sheppard, "Aluminum nitride: A versatile but challenging material," *Ceramic Bulletin,* vol. 69, no. 11, pp. 1881–1891, 1990.

[2] G. A. Slack, "Nonmetallic crystals with high thermal conductivity," *J. Phys. Chem. Solid,* vol. 31, p. 321, 1973.

[3] Y. Kurokawa, K. Utsumi, H. Takamizwa, T. Kamata, and S. Noguchi, "AlN substrates with high thermal conductivity," *IEEE Trans. Comp., Hybrids, Manuf. Technol.,* vol. CHMT-8, no. 6, pp. 247–252, 1985.

[4] D. D. Marchant and T. E. Nemecek, "Aluminum nitride: Preparation, processing, and properties," *Ceramic Substrates and Packages for Electronic Applications,* Advances in Ceramics, Vol. 26, M. F. Yan, K. Niwa, H. M. O'Bryan, and W. S. Young, eds. American Ceramic Society, 1987, pp. 19–54.

[5] A. J. Blodgett, "A multilayer ceramic multichip module," *IEEE Trans. Comp., Hybrids, Manuf. Technol.,* vol. CHMT-3, pp. 624–629, 1980.

[6] N. Iwase, K. Anzai, K. Shinozaki, O. Hirao, T. D. Thanh, and Y. Sugiura, "Thick film and direct bond copper forming technology for aluminum nitride substrate," *IEEE Trans. Comp., Hybrids, Manuf. Technol.,* vol. CHMT-8, no. 2, pp. 253–258, 1985.

[7] Y. S. Sun *et al.,* "A new hybrid power technique utilizing a direct copper to ceramic bond," *IEEE Trans. Electron Devices,* vol. ED-23, no. 8, pp. 961–967, 1967.

[8] J. Wynschenk, "Electroless copper plating: Chemistry and maintenance," *Plating and Surface Finishing,* vol. 70, no. 1, pp. 28–29, 1983.

[9] P&SF Report, "Developments in electroless plating," *Plating and Surface Finishing,* vol. 71, no. 2, pp. 36–39, 1984.

[10] C. H. Ting and M. Paunovic, "Selective electroless metal deposition for integrated circuit fabrication," *J. Electrochem. Soc.,* vol. 136, no. 2, pp. 456–462, 1989.

[11] C. J. Bartlett, R. D. Rust, and R. J. Rhodes, "Electroless copper plating of multilayer printed circuit boards," *Plating and Surface Finishing,* vol. 65, no. 7, pp. 36–41, 1978.

[12] J. Henry, "Electroless plating: Part III—copper," *Metal Finishing,* vol. 82, no. 11, pp. 47–48, 1984.

[13] A. Hung, "Kinetic of electroless copper deposition with hypophosphite as a reducing agent," *Plating and Surface Finishing,* vol. 75, no. 4, pp. 74–77, 1988.

[14] E. B. Saubestre, "Stabilizing electroless copper solutions," *Plating,* vol. 59, no. 6, pp. 563–566, 1972.

[15] A. Molenaar, M. F. E. Hddrinet, and L. K. H. Van Beek, "Kinetics

of electroless copper plating with EDTA as the complexing agent for cupric ions," *Plating,* vol. 61, no. 3, pp. 238–242, 1974.

[16] F. J. Muzzi, "Accelerating the rate of electroless copper plating," *Plating and Surface Finishing,* vol. 70, no. 1, pp. 51–54, 1983.

[17] J. Duffy, L. Pearson, and M. Paunovic, "The effect of pH on electroless copper deposition," *J. Electrochem. Soc.,* vol. 130, no. 4, pp. 876–880, 1983.

[18] A. Hung, "Effect of thiourea and guanidine hydrochloride on electroless copper plating," *J. Electrochem. Soc.,* vol. 123, no. 5, pp. 1047–1049, 1976.

[19] M. Pounovic and R. Arndt, "The effect of some additives on electroless copper deposition," *J. Electrochem. Soc.,* vol. 130, no. 4, pp. 794–799, 1983.

[20] E. K. Yung and L. T. Romamankiw, "Plating of copper into through-holes and vias," *J. Electrochem. Soc.,* vol. 136, no. 1, pp. 206–215, 1989.

[21] M. Schlesinger and J. Kisel, "Effect of Sn(II)-based sensitizer adsorption in electroless deposition," *J. Electrochem. Soc.,* vol. 137, no. 6, 1658–1661, 1990.

[22] J. F. D'Amic, "Selective electroless metal deposition using patterned photo-oxidation of Sn(II) sensitized substrate," *J. Electrochem. Soc.,* vol. 118, no. 10, pp. 1695–1699, 1971.

[23] C. E. Baumgartner, "Photo-selective electroless metal deposition following light absorption by titanate ceramics," *J. Electrochem. Soc.,* vol. 137, no. 11, pp. 2343–2346, 1980.

[24] T. Osaka and H. Negasaka, "An electron diffraction study on mixed $PdCl_2$ catalysts for electroless plating," *J. Electrochem. Soc.,* vol. 127, no. 11, pp. 2343–2346, 1980.

[25] T. Osaka and H. Takematsu, "A study on activation and acceleration by mixed $PdCl_2/SnCl_2$ catalysts for electroless metal deposition," *J. Electrochem. Soc.,* vol. 127, no. 5, pp. 1021–1029, 1980.

[26] N. Feldstein, "Electron microscope investigation of mixed stannous chloride/palladium chloride catalysts for plating dielectric substrates," *J. Electrochem. Soc.,* vol. 121, no. 6, pp. 738–744, 1974.

[27] D. W. Baudrand, "Cleaning and preparation of ceramic and metallized ceramic materials for plating," *Plating and Surface Finishing,* vol. 71, no. 10, pp. 72–75, 1984.

[28] H. Honma and K. Kanemitsu, "Electroless nickel plating on alumina ceramics," *Plating and Surface Finishing,* vol. 74, no. 9, pp. 62–67, 1987.

[29] H. Honma and Y. Kouchi, "Direct electroless copper plating on alumina ceramics," *Plating and Surface Finishing,* vol. 77, no. 6, pp. 54–58, 1990.

[30] L. G. Bhatgadde and S. Mahapatra, "Adhesion of electroless copper on alumina," *Metal Finishing,* vol. 85, no. 1, pp. 55–57, 1987.

[31] J. Muir and J. R. Williams, "Copper metallization of conventional and alternate ceramics," in *ISHM'88 Proc.,* 1988, pp. 196–202.

[32] W. K. Jones, "Evaluation of copper plated ceramic substrates," in *ISHM'88 Proc.,* 1988, pp. 164–168.

[33] R. J. Geckle, "Metallurgical changes in TiN-lead platings due to heat aging," *IEEE Trans. Comp., Hybrids, Manuf. Technol.,* vol. CHMT-14, no. 4, pp. 691–697, 1991.

[34] K. Utsumi, "Metallization of AlN ceramics by electroless Ni-P plating," *J. Electrochem. Soc.,* vol. 133, no. 11, pp. 2345–2349, 1986.

[35] T. Osaka, T. Asada, E. Nakajima, and I. Koiwa, "Chemical etching properties of high thermal conductive AlN ceramics for electroless Ni-P metallization," *J. Electrochem. Soc.,* vol. 135, no. 10, pp. 2578–2581, 1988.

[36] B. S. Chiou, G. H. Chang, and J. G. Duh, "Metallization of AlN substrates by electroless Cu plating," *Plating and Surface Finishing,* 80, pp. 65–68, 1993.

[37] J. H. Chang, M.S. thesis, National Tsing Hua University, Hsinchu, Taiwan, 1992.

[38] Y. Okinaka and H. K. Straschil, "The effect of inclusions on the ductility of electroless copper deposits," *J. Electrochem. Soc.,* vol. 133, no. 12, pp. 2608–2615, 1986.

J. H. Chang, photograph and biography not available at the time of publication.

J. G. Duh, photograph and biography not available at the time of publication.

B. S. Chiou, photograph and biography not available at the time of publication.